VERTICAL WELL PRESSURE AND PRESSURE DERIVATIVE ANALYSIS FOR BINGHAM FLUIDS IN HOMOGENEOUS RESERVOIRS

ANÁLISIS DE PRESIÓN Y DERIVADA DE PRESIÓN PARA FLUIDOS BINGHAM EN POZOS VERTICALES EN YACIMIENTOS HOMOGENEOS

JAVIER A. MARTINEZ
Programa de Ingeniería de Petróleos, Universidad Surcolombiana, Researcher, j_martinez70@hotmail.com

FREDDY H. ESCOBAR
Programa de Ingeniería de Petróleos, Universidad Surcolombiana, Professor, fescobar@usco.edu.co

MATILDE MONTEALEGRE
Programa de Ingeniería de Petróleos, Universidad Surcolombiana, Professor, matildelina2005@hotmail.com

Received for review September 14 th, 2009, accepted October 8th, 2010, final version October 14 th, 2010

ABSTRACT: This paper presents a technique for interpreting the behavior of pressure and pressure derivative for a Bingham-type fluid in a homogeneous reservoir drained by a vertical well using the TDS technique, by observing the influence of the minimum pressure gradient which characterizes this behavior, and characteristic points which are used for estimating formation permeability, drainage area, and skin factor. The pressure derivative for Bingham Non-Newtonian fluids is presented in the literature for the first time. The higher the minimum pressure gradient, the more asymmetrically concave the pressure derivative becomes. Also, it was observed in closed systems that the late unit-slope pressure derivative coincides with the same one for Newtonian fluids.

KEY WORDS: Bingham fluid, pressure gradient, yield stress, shear stress, shear rate

RESUMEN: Este trabajo presenta una técnica de interpretación del comportamiento de la presión y derivada de presión para un fluido tipo Bingham en un yacimiento homogéneo drenado por un pozo vertical, aplicando la técnica TDS observando la influencia del gradiente mínimo de presión que caracteriza este comportamiento y puntos característicos con el propósito de calcular la permeabilidad, el área de drenaje y el factor de daño de la formación. Es la primera vez que se presenta en la literatura la derivada de presión para estos fluidos. Entre mayor se hace el mínimo gradiente de presión la derivada se hace asimétricamente más cóncava hacia arriba. También se observó que en sistemas cerrados la pendiente unitaria tardía que se desarrolla en la derivada de presión coincide con la misma de fluidos Newtonianos.

PALABRAS CLAVES: Fluido Bingham, gradiente de presión, esfuerzo de cedencia, esfuerzo de corte, rata de corte.

1. INTRODUCTION

Flow of non-Newtonian fluids through porous media is encountered in many subsurface systems involving underground natural resource recovery or storage projects. Laboratory experiments and field tests indicate that certain fluids exhibit a Bingham-type non-Newtonian behavior in porous media. In these cases, flow only takes place once the applied pressure gradient exceeds a certain minimum value called the threshold pressure gradient. The flow of oil in many heavy oil reservoirs does not follow Darcy's law but may be approximated by a Bingham Fluid.

A few studies of well pressure behavior in vertical wells have been recently conducted on the behavior of the non-Newtonian fluid approaching the power law model in vertical wells using both the *TDS* technique [1] and type-curve matching [2] and similarly for horizontal wells with non-Newtonian Bingham fluids [3].

In this work, the model governing the behavior of the flow of a non-Newtonian Bingham fluid in a closed porous media drained by a vertical well, [4], was numerically solved, see Appendix A. Once the pressure and pressure derivative was generated, the interpretation methodology was obtained by following the *TDS* philosophy to determine reservoir permeability, skin factor and drainage area, and tested through synthetic examples previously employed by [4].

2. BINGHAM FLUID AND RHEOLOGICAL MODEL

As a special kind of non-Newtonian fluid, Bingham fluids (or Bingham plastics) exhibit a finite yield stress at zero shear rates. There is no gross movement of fluids until the yield stress, τ_y, is exceeded. Once this is accomplished, it is also required to cut efforts to increase the shear rate, i.e. they behave as Newtonian fluids.

These fluids behave as a straight line crosses the *y* axis in $\tau = \tau_y$, when the shear stress, τ is plotted against the shear rate, $\dot{\gamma}$ in Cartesian coordinates. The characteristics of these fluids are defined by two constants: the yield, τ_y, which is the stress that must be exceeded for flow to begin, and the Bingham plastic coefficient, μ_B. The rheological equation for a Bingham plastic is, [5]:

$$\tau = \tau_y + \mu_B \dot{\gamma} \tag{1}$$

The Bingham plastic concept has been found to closely approximate many real fluids existing in porous media, such as paraffinic oils, heavy oils, drilling muds and fracturing fluids, which are suspensions of finely divided solids in liquids. Laboratory investigations have indicated that the flow of heavy-oil in some fields has non-Newtonian behavior and approaches the Bingham type.

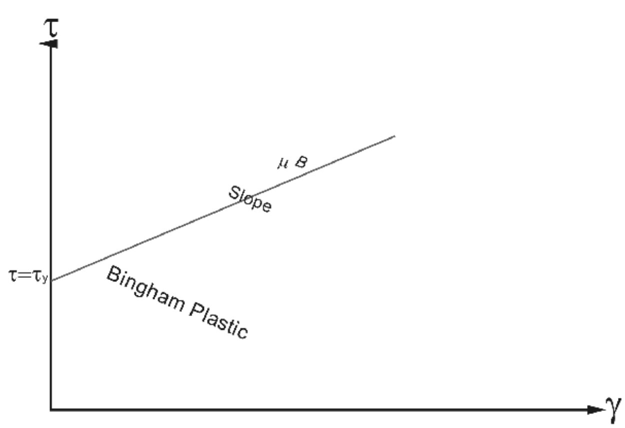

Figure 1. Graphic Representation of Bingham fluid, [5]

For a phenomenological description of flow in porous media, some equivalent or apparent viscosities for non-Newtonian fluid flow are needed in Darcy's equation. Therefore, many experimental and theoretical studies have investigated rheological models or correlations of apparent viscosities and flow properties for a given non-Newtonian fluid and porous material. For flow problems in porous media involving non-Newtonian Bingham fluids, the formulation of Darcy's law has been modified to:

$$\vec{u} = -\frac{k}{\mu_B}\left(1 - \frac{G}{|\nabla P|}\right)\nabla p \quad \text{for} \quad |\nabla P| > G \tag{2a}$$

and,

$$\vec{u} = 0 \quad \text{for} \quad |\nabla P| \le G \tag{2b}$$

Where, G is the pressure gradient corresponding to the yield stress in a porous medium. The above conditions show that in this type of fluid, there is no flow until $|\nabla P|$ exceeds the minimum pressure gradient, G. The two Bingham-fluid parameters, G and μ_B, should be determined by laboratory experiments or by a well test for a porous medium flow problem. For heavy oils, a reasonable value of G is in the order of 10^4 Pa/m (0.44 psi/ft).

[4] presented the governing equation for the problem we are dealing with. [4] also provided a complex analytical integral solution which requires numerical integration. [4] interpreted the pressure tests by numerical solutions and regression analysis, which means matching the well pressure response to the simulator response.

3. MATHEMATICAL FORMULATION

The problem considered here, presented by [4], involves the production of a Bingham fluid from a fully penetrating vertical well in a horizontal reservoir of constant thickness; the formation is saturated only with the Bingham fluid. The basic assumptions are:

1. Isothermal, isotropic, and homogeneous formation.
2. Single-phase horizontal flow without gravity effects.
3. Darcy's law applies (Eq. 2)
4. Constant fluid properties and formation permeability.

The governing flow equation can be derived by combining the modified Darcy's law with the continuity equation and is expressed in a radial coordinate system as:

$$\frac{k}{r}\frac{\partial}{\partial r}\left[\frac{\rho(P)}{\mu_B}r\left(\frac{\partial P}{\partial r}-G\right)\right]=\frac{\partial}{\partial t}\left[\rho(P)\phi(P)\right] \quad (3)$$

The density of the Bingham fluid, $\rho(P)$, and the porosity of the formation, $\phi_i = \phi(P)$, are functions of pressure only, so the solution of the Eq. 3 is:

$$\frac{1}{r}\frac{\partial}{\partial r}\left[r\left(\frac{\partial P}{\partial r}-G\right)\right]=\frac{\phi\mu_B c_t}{k}\frac{\partial P}{\partial t} \quad (4)$$

The initial condition is:

$$P(r,t=0)=P_i, \qquad r \geq r_w$$

At the wellbore inner boundary, $r = r_w$, the fluid is produced at a given production rate, q, then the inner boundary condition is:

$$q=2\pi rh\frac{k}{\mu_B}\left(\frac{\partial P}{\partial r}-G\right)_{r=r_w} \quad (5)$$

4. FUNDAMENTAL EQUATIONS

The dimensionless pressure P_D, the dimensionless time t_D, the dimensionless radius, r_D and the dimensionless pressure gradient, G_D (conveniently introduced here) are expressed as:

$$P_D=\frac{kh\Delta P}{141.2q\mu_B B} \quad (6)$$

$$t_D=\frac{0.0002637kt}{\phi\mu_B c_t r_w^2} \quad (7)$$

$$r_D=\frac{r}{r_w},\ r_{eD}=\frac{r_e}{r_w} \quad (8)$$

$$G_D=\frac{Gr_w kh}{141.2q\mu_B B} \quad (9)$$

5. INTERPRETATION METHODOLOGY

The way the interpretation equations are formulated follows the philosophy of the *Tiab´s Direct Synthesis*, *TDS*, Technique, introduced by [6].

1) For radial flow and Newtonian fluid, the dimensionless pressure derivative is:

$$\left(t_D*P_D'\right)_r=\frac{kh\left(t*\Delta P'\right)_r}{141.2q\mu_B B}=0.5 \quad (10)$$

For a Bingham-type non-Newtonian fluid, this behavior changes by observing that there is a point where the dimensionless pressure derivative is high and this increases with an increase of G_D and the reservoir radius, Figs. 2 and 3. Fig. 4 shows the trend between the dimensionless outer radius and the dimensionless derivative pressure maximum for various G_D. The slope of each line is the product $0.20536G_D$. So by grouping all the straight lines in one, we obtain the following relationship:

$$\left(t_D*P_D'\right)_{r,max}=0.5+0.20536G_D r_{eD} \quad (11)$$

$$\left(t_D*P_D'\right)_{r,max}-0.20536G_D r_{eD}=0.5 \quad (12)$$

Alter plugging the dimensionless quantities in the above expressions, it yields, respectively:

$$\frac{kh}{141.2q\mu B}\left[\left(t*\Delta P'\right)_{r,max}-0.20536Gr_e\right]=0.5 \text{ then,}$$

$$k=\frac{70.6q\mu_B B}{h\left[\left(t*\Delta P'\right)_{r,max}-0.20536Gr_e\right]} \quad (13)$$

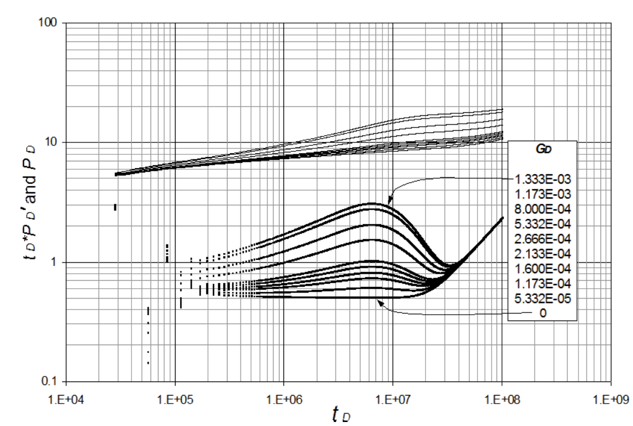

Figure 2. Dimensionless pressure and derivative pressure for $r_{eD} = 9375$

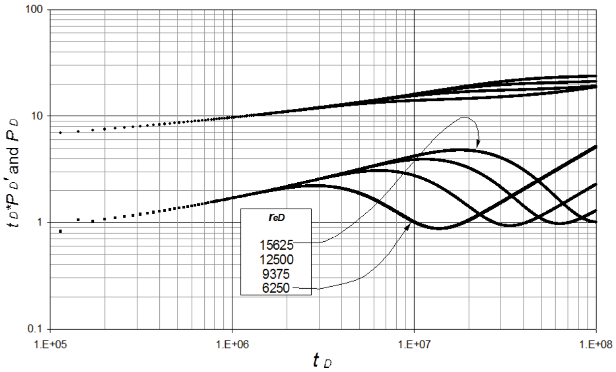

Figure 3. Dimensionless pressure and derivative pressure for $G_D = 1.333\text{x}10^{-3}$

2) The behavior of the dimensionless pressure is added to the equation for radial flow and Newtonian fluid to produce an additional quantity we call "Bingham effect" which does not depend upon reservoir size, Fig. 5.

$$P_{Dr} = 0.5\left[ln\, t_D + 0.80907 + 2s\right] + B_{eff} \tag{14}$$

where:

$$B_{eff} = 1.69602 G_D t_D^{0.50304} \tag{15}$$

3) The skin factor, *s*, can be obtained by dividing Eq. 14 with Eq. 12:

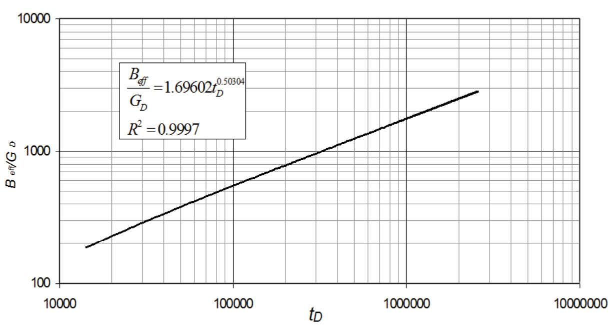

Figure 5. Correlation for the "Bingham effect"

$$s = \frac{1}{2}\left[\frac{\Delta P_{r,max}}{(t*\Delta P')_{r,max} - 0.20536 G r_e} - ln\left(\frac{k t_{r,max}}{\phi \mu_B c_t r_w^2}\right) + 7.43\right] - B_{eff} \tag{16}$$

In *G* = 0 the fluid is Newtonian which leads to the normal equations for obtaining permeability and skin factor as presented by [6].

4) As observed in Fig. 2, the late pressure derivative coincides with that of a Newtonian fluid. Then, according to [7], the reservoir drainage area can be estimated from any convenient point during the late pseudosteady state derivative.

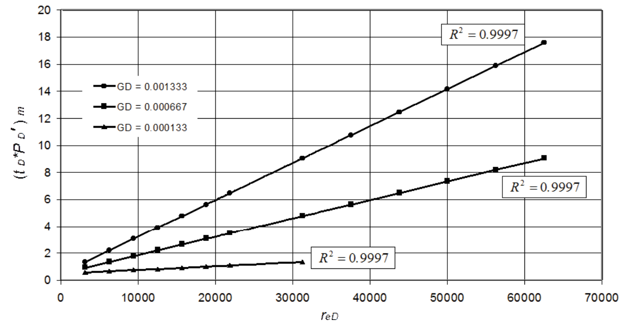

Figure 4. Relationship between the dimensionless radius and the dimensionless derivative pressure at its peak

$$A = \frac{0.234 q B t_{pss}}{\phi c_t h (t*\Delta P')_{pss}} \tag{17}$$

Which can be applied for t = 1 hr, extrapolating if necessary, so Eq. 17.a becomes:

$$A = \frac{0.234 q B}{\phi c_t h (t*\Delta P')_{p1}} \tag{18}$$

Permeability can also be determined by relating the dimensionless outer radius with the maximum dimensionless time. This relationship works for any G_D as shown in Fig. 6. The resulting equation is:

$$k = \frac{278.3817710 r_e^{2.0} \phi \mu_B c_t}{t_{r,max}} \tag{19}$$

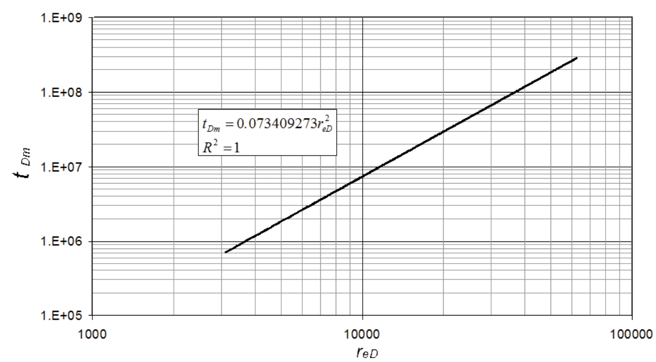

Figure 6. Relationship between the dimensionless outer radius and the maximum dimensionless time

5) Eqs. 13 and 19 are functions of the external reservoir radius. When the late pseudosteady-state flow is not developed, then permeability is obtained by equating Eqs. 14 and 19. This yields:

$$k = \frac{0.20536 k^{1.5} t_{r,max}^{0.5} G}{(t*\Delta P')_{r,max}\left(278.3817710 \phi \mu_B c_t\right)^{0.5}} + \frac{70.6 q \mu B}{h (t*\Delta P')_{r,max}} \tag{20}$$

Eq. 20 is solved iteratively using the Newton-Raphson method (or any other) by choosing an initial value of permeability, until the difference between the new and previous value is less than 0.001.

$$f(k)=\frac{0.20536k^{1.5}t_{r,max}^{0.5}G}{(t*\Delta P')_{r,max}\left(278.3817710\phi\mu_B c_t\right)^{0.5}}+\frac{70.6q\mu B}{h(t*\Delta P')_{r,max}}-k \qquad (21)$$

$$f'(k)=\frac{0.30804k^{0.5}t_{r,max}^{0.5}G}{(t*\Delta P')_{r,max}\left(278.3817710\phi\mu_B c_t\right)^{0.5}}-1 \qquad (22)$$

$$k_{n+1}=k_n-\frac{f(k)}{f'(k)} \qquad (23)$$

6) Fig. 7 shows a relation between the dimensionless minimum pressure gradient and the Cartesian slope of the pressure derivative values during the radial flow regime. If there is no peak in the derivative pressure, obtaining the Cartesian slope of the derivative pressure against time, we can obtain the permeability.

$$k=\frac{141.2q\mu B}{Gr_w h}\left(7.9146325\times10^{-6}+8.3684407\times10^{-5}m^{0.9996726}\right) \qquad (24)$$

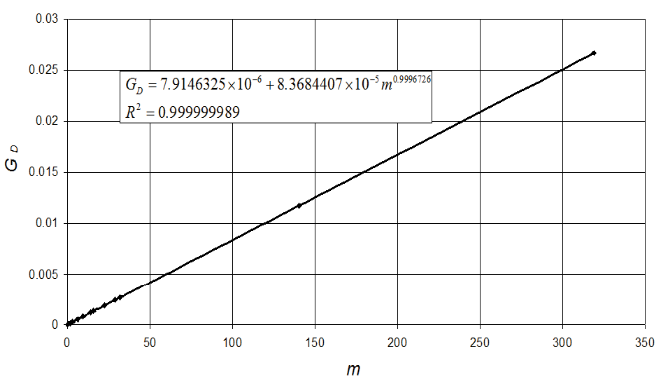

Figure 7. Relationship between Cartesian slope from the pressure derivative during radial flow and dimensionless pressure gradient

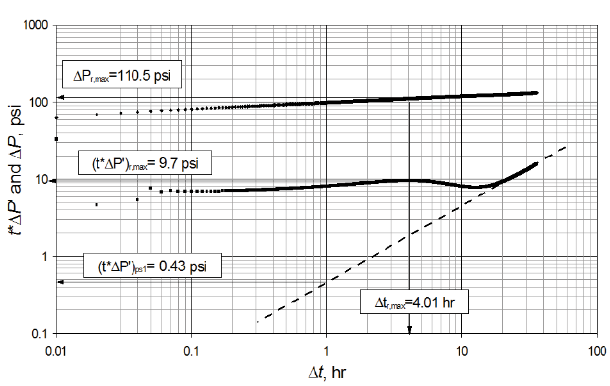

Figure 8. Pressure and pressure derivative for example 1

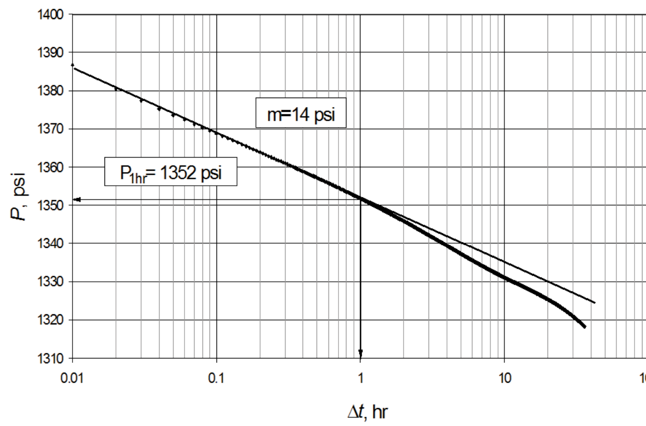

Figure 9. Semilog plot of pressure vs. time for example 1

6. EXAMPLES

6.1. Synthetic example 1

With the information taken from [9] obtain the formation permeability and the skin factor from a reservoir that produces a Bingham-type fluid with a G = 0.0044 psi/ft (100 Pa/m)

P_i = 1450 psi q = 272 STB/D h = 3.2 ft

ϕ = 20 % k = 1000 md μ_B = 1 cp

r_w = 0.32 ft B = 1 rb/STB c_t = 4.52x10^{-6} psi^{-1}

SOLUTION

From Fig. 8, the following information is read:

$\Delta P_{r,\ máx.}$ = 110.5 psi $(t*\Delta P')_{r,\ máx.}$ = 9.7 psi

$(t*\Delta P')_{p1}$ = 0.43 psi $t_{r,máx}$ = 4.01 hr

The drainage area is obtained from Eq. 18 using information from the late pseudosteady-state regime:

$$A=\frac{0.234*272*1}{0.2*4.52\times10^{-6}*3.2*0.43}=51167925.8\ \text{ft}^2$$

Assuming a circular reservoir shape, the reservoir radius, r_e, is 4035.75 ft.

Formation permeability is estimated from Eq. 14:

$$k=\frac{70.6*272*1*1}{3.2*\left[9.7-0.20536*0.0044*4035.75\right]}$$

$$k=991.35\ \text{md}$$

The dimensionless minimum pressure gradient, Eq. 9, is:

$$G_D = \frac{0.0044*0.32*991.35*3.2}{141.2*272*1*1} = 1.163\times10^{-4}$$

Now, skin factor can be estimated from Eq. 16:

$$s = \frac{1}{2}\left[\frac{110.5}{9.7-0.205*0.0044*4035.75} - ln\left(\frac{991.35*4.01}{0.2*1*4.52\times10^{-6}*0.32^2}\right)+7.43\right]$$

$$-1.7*3.634\times10^{-5}*\left(\frac{0.0002637*991.35*4.01}{0.2*1*4.52\times10^{-6}*0.32^2}\right)^{0.50304}$$

$$s = -0.097$$

Eq. 19 is employed to estimate formation permeability as follows:

$$k = \frac{278.4*4035.75^{2.0}*0.2*1*4.52\times10^{-6}}{4.01} = 1022.15 \text{ md}$$

Since G_D is small enough for the application of the semilog (conventional) straight-line method, the semilog slope is obtained from Fig. 9, then:

$$k = \frac{162.6q\mu B}{mh} = \frac{162.6*272*1*1}{14.0*3.2} = 987.2 \text{ md}$$

$$s = 1.1513\left[\frac{P_{1hr}-P_i}{m} - \log\left(\frac{k}{\phi\mu c_t r_w^2}\right)+3.23\right]$$

$$s = 1.1513\left[\frac{1352-1450}{-14} - \log\left(\frac{987.2}{0.2(1)(4.52\times10^{-6})0.32^2}\right)+3.23\right]$$

$$s = 0.24$$

These last two equations were presented in a monograph published by [8]. However, the conventional method or straight –line method is difficult to apply in this type of systems, especially when G_D > 5.33x10^{-4}, since no straight line is formed during radial flow, as seen in Fig. 10.

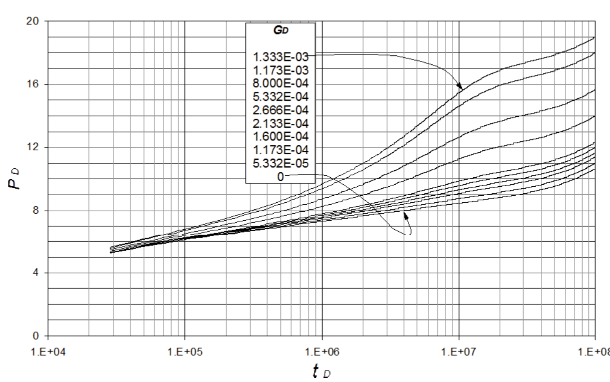

Figure 10. Dimensionless semilog plot

6.2. Synthetic example 2

A drawdown test for a well centered in a closed circular reservoir with a *G* = 0.44 psi/ft was generated with the information given below. Use the *TDS* technique to interpret this test.

P_i = 3000 psi q = 300 STB/D h = 50 ft

k = 300 md μ_B = 3 cp r_w = 0.35 ft

B = 1.25 rb/STB ϕ = 20 % c_t = 2x10^{-6} psi^{-1}

SOLUTION

From Fig. 10, the information below was read:

$\Delta P_{r,\, máx.}$ = 1128 psi $(t*\Delta P')_{r,\, máx.}$ = 456 psi

$t_{r,máx}$ = 25.0 hr

As seen in Fig. 10, the late pseudosteady-state regime was not developed for this test, so a trial-and-error procedure has to be used with Eqs. 20-22 starting with a permeability value of 400 md:

$$f(k) = 0.05714k^{1.5} + 3.4836 - k$$

$$f'(k) = 0.08571k^{0.5} - 1$$

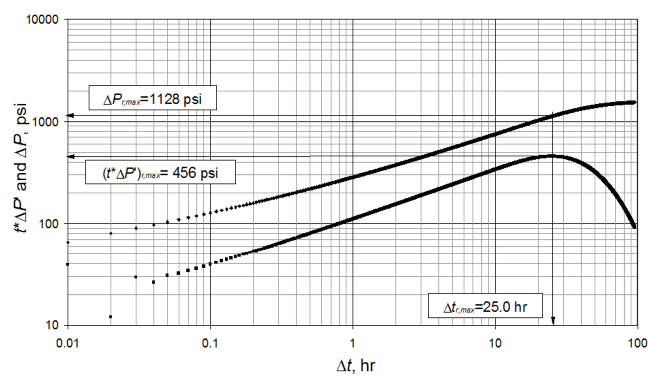

Figure 11. Pressure and pressure derivative for example 2

A summary of the following computations is shown below:

N	k_n	*F*(*k*)	*F'*(*k*)	-*F*(*k*)/*F'*(*k*)
0	400	60.603	0.7142	-84.855
1	315.1447	8.0114	0.5215	-15.360
2	299.7838	0.2870	0.4840	-0.593
3	299.1907	0.0004	0.4825	-0.0009
4	299.1898	0.0000	0.4825	0.00000
5	299.1898	0	0.4825	0

$k \approx 299.2$ md. Reservoir size is needed for the estimation of skin factor. Then, solving for r_e from Eq. 19:

$$r_e = \sqrt{\frac{299.2*25}{278.4*0.18*3*2\times10^{-6}}} = 4987.82\,\text{ft}$$

The minimum dimensionless pressure gradient is obtained by means of Eq. 9. Afterwards, skin factor is calculated from Eq. 16,

$$G_D = \frac{0.44*0.35*299.2*50}{141.2*300*3*1.25} = 0.0145$$

$$s = \frac{1}{2}\left[\frac{1128}{456 - 0.205*0.44*4987.82} - ln\left(\frac{299.2*25}{0.18*3*2\times10^{-6}*0.35^2}\right) + 7.43\right]$$

$$-1.7*0.0145*\left(\frac{0.0002637*299.2*25}{0.18*3*2\times10^{-6}*0.35^2}\right)^{0.50304}$$

s = -2.27

7. COMMENTS ON THE RESULTS

The two synthetic examples presented have shown that the proposed methodology and developed equations/correlations work very well. In the first example, permeability was estimated with an absolute deviation error less than 2.2 %. In the other example the deviation was 0.26 %. Although, for the first example, a good permeability value was obtained from the conventional technique since the value of the minimum pressure gradient was small. This means that the semilog straight line is still seen and representative. For the first example, the skin factors agree well. There is no comparison point for the second example.

CONCLUSIONS

1. A new formulation for estimating permeability and skin factor in non Newtonian fluids in vertical wells using the *TDS* technique is presented. Although, some correlations are involved, their correlation coefficient is practically one in all the cases.
2. A “Bingham effect” was introduced here on the dimensionless pressure variation. To maintain the same flow rate, the wellbore pressure decrease more rapidly as the minimum pressure gradient increases.
3. As the minimum pressure gradient increases, the pressure derivative becomes asymmetrically more concave, displaying a maximum or “peak” point which is taken as a characteristic feature which is used for well test interpretation. The shape of the pressure derivative is also a function of reservoir size. As the reservoir size increases the time position of the peak increases. The time at which the pressure derivative is maximum is the same for any G_D value and the same size of the reservoir.
4. All the pressure derivative curves for the same reservoir radius tend to display the same pseudosteady state, which is employed for estimating the reservoir drainage area.

NOMENCLATURE

A	Area, ft^2
B	Oil formation factor, rb/STB
c_t	Total system compressibility, 1/psi
G	Minimum pressure gradient, psi/ft
G_D	Dimensionless pressure gradient
h	Thickness formation, ft
k	Permeability, md
M	Cartesian slope of the pressure derivative trend during radial flow regime
P	Pressure, psi
P_D	Dimensionless pressure
P_i	Initial reservoir pressure, psi
P_{wf}	Well flowing pressure, psi
q	Oil Rate, bbl/D
q_w	Well flow rate, positive means injection, positive means production
r_D	Dimensionless radius
r_e	Reservoir radius, ft
r_w	Wellbore radius, ft
s	Skin factor
t	Time, hr
t_D*P_D'	Dimensionless logarithmic pressure derivative
$t*\Delta P'$	Pressure derivative, psi
t_D	Dimensionless time

SUFFIXES

D	Dimensionless
pss	Any point during late pseudosteady state regime
$p1$	Pressure derivative on the pseudosteady state line read at 1 hr
r, max	Maximum during radial flow regime

GREEK SYMBOLS

Δ	Change, drop
Δt	Flow time, hr
Δr	Cell spacing in the radial direction, ft
ρ	Density, lbm/ft^3
ϕ	Porosity, fraction
μ_B	Bingham plastic Coefficient, cp

REFERENCES

[1] KATIME, I., and TIAB, D., 2001. Analysis of Pressure Transient Test of Non-Newtonian Fluids in Infinite Reservoir and in the Presence of a Single Linear Boundary by the Direct Synthesis Technique. Paper SPE 71587 Paper SPE 71587 prepared for presentation at the 2001 SPE Annual Technical Conference and Exhibition held in New Orleans, Louisiana, 30 Sept.–3 Oct.

[2] IGBOKOYI, A. and TIAB, D. 2007. New Type Curves for the Analysis of Pressure Transient Data Dominated by Skin and Wellbore Storage – Non Newtonian Fluid. Paper SPE 106997 presented in the Productions Operation Symposium held in Oklahoma City, OK, March 31-April 4.

[3] OWAYED, J. F. and TIAB, D., 2008. Transient pressure behavior of Bingham non-Newtonian fluids for horizontal wells. Journal of Petroleum Science and Engineering, Volume 61, Issue 1, April 2008, Pages 21-32.

[4] WU, Y.S., 1990. Theoretical Studies of Non-Newtonian and Newtonian Fluid Flow Through Porous Media. Ph.D. dissertation, U. of California, Berkeley.

[5] BEAR, J., 1972. Dynamics of Fluids in Porous Media. Elsevier Science Publishers, New York City.

[6] TIAB, D., 1995. Analysis of Pressure and Pressure Derivative without Type-Curve Matching: 1- Skin Factor and Wellbore Storage. Journal of Petroleum Science and Engineering 12 (1995), p. 171-181.

[7] CHACON, A., DJEBROUNI, A., and TIAB, D., 2004. Determining the Average Reservoir Pressure from Vertical and Horizontal Well Test Analysis Using the Tiab's Direct Synthesis Technique. Paper SPE 88619 presented at the SPE Asia Pacific Oil and Gas Conference and Exhibition held in Perth, Australia, 18–20 October 2004.

[8] MATHEWS, C.S. and RUSSELL, D.G., 1967. Pressure Buildup and Flow Tests in Wells. SPE Monograph Vol. 1. 1967.

[9] WU, Y.S, PRUESS, K. and WITHERSPOON, P.A., 1992. Flow and Displacement of Bingham Non-Newtonian Fluids in Porous Media. SPE Reservoir Engineering. August 1992, p. 369-376.

APPENDIX A. NUMERICAL SOLUTION

A logarithmic grid was used to solve the problem. The numerical solution was successfully tested for cases of $G = 0$ and, also, compared to the graphical solutions presented by Wu et al. (1992). The discretization process of Eq. 4 follows:

$$\frac{1}{r_i(\Delta r)_i}\left\{r_{i+\frac{1}{2}}\left(\frac{\left(P_{i+1}-P_i\right)^{n+1}}{(\Delta r)_{i+\frac{1}{2}}}-G\right)-r_{i-\frac{1}{2}}\left(\frac{\left(P_i-P_{i-1}\right)^{n+1}}{(\Delta r)_{i-\frac{1}{2}}}-G\right)\right\}=\frac{P_i^{n+1}-P_i^n}{\eta\Delta t} \quad \text{(A.1)}$$

Where $\eta = \frac{k}{\phi\mu_B c_t}$

Solving for the transmissibilities, it yields:

$$T_{i+\frac{1}{2}}^{n+1}\left(P_{i+1}^{n+1}-P_i^{n+1}-G\Delta r_{i+1/2}\right)-T_{i-1/2}^{n+1}\left(P_i^{n+1}-P_{i-1}^{n+1}-G\Delta r_{i-1/2}\right)\pm$$

$$q_w = \frac{24V r_i\phi c_t}{5.615B\Delta t}\left(P_i^{n+1}-P_i^n\right) \quad \text{(A.2)}$$

Where $V_{ri} = \pi\left(r_{i+1/2}^2 - r_{i-1/2}^2\right)h$

It should be clarified that for the first grid point, $r_{i-1/2}=r_w$ and for the last grid point (boundary), $r_{i+1/2}=r_e$. Assuming constant petrophysical properties, the transmissibilities are:

$$T = T_{i+1/2} = T_{i-1/2} = 0.00708\frac{hk}{\mu B}\frac{1}{ln\alpha} \quad \text{(A.3)}$$

Where $\alpha = \left(r_e / r_w\right)^{1/(N-1)}$

Using the above relationships, the final equation applied to each gridpoint is:

$$TP_{i-1}^{n+1} - \left(2T+F\right)P_i^{n+1} + TP_{i+1}^{n+1} = -FP_i^n + TG\left(\Delta r_{i+1/2} - \Delta r_{i-1/2}\right) \pm q_w \quad \text{(A.4)}$$

Where, $a = c = T$, $b = -2T - F$, and

$$d = -FP_i^n + TG\left(\Delta r_{i+1/2} - \Delta r_{i-1/2}\right) \pm q_w$$

$$F = \frac{24V r_i\phi c_t}{5.615B\Delta t}$$

Application of Eq. A.4 to the first and last gridpoint, respectively, it will result:

$$-\left(T+F\right)P_i^{n+1} + TP_{i+1}^{n+1} = -FP_i^n + TG\Delta r_{i+1/2} \pm q_w$$

$$TP_{i-1}^{n+1} - \left(T+F\right)P_i^{n+1} = -FP_i^n - TG\Delta r_{i-1/2}$$

The final tri-diagonal matrix system is solved by the Thomas algorithm.